Metabolic profiling of three Brachypodium species reveals different adaptive strategies to ammonium stress

Marlon de la Peña, Izargi Vega-Mas, Gaëtan Glauser, Yves Gibon, Daniel Marino, María Begoña González-Moro

Plant Science 360 (2025) 112684

Contents lists available at ScienceDirect

Plant Science

journal homepage: www.elsevier.com/locate/plantsci

Metabolic profiling of three Brachypodium species reveals different adaptive strategies to ammonium stress

Marlon De la Peña [a,1], Izargi Vega-Mas [a], Gaëtan Glauser [b], Yves Gibon [c], Daniel Marino [a,*], María Begoña González-Moro [a,*]

[a] Department of Plant Biology and Ecology, University of the Basque Country (UPV/EHU), Leioa E-48940, Spain
[b] Neuchâtel Platform of Analytical Chemistry, University of Neuchâtel, Avenue de Bellevaux 51, Neuchâtel 2000, Switzerland
[c] Université de Bordeaux, INRAE, UMR Biologie du Fruit et Pathologie, Bordeaux Metabolome, Villenave d'Ornon F-33140, France

ARTICLE INFO

Keywords:
Ammonium
Brachypodium
Metabolomics
Natural variation
Nitrate
Nitrogen metabolism
Nutritional stress

ABSTRACT

Nitrogen (N) use efficiency (NUE) in crops is a critical challenge, as only 40 % of applied nitrogen is typically recovered at harvest. Ammonium-based nutrition is proposed as a strategy to increase NUE in agrosystems. However, crops display better performance when growing with a nitrate-based nutrition. To advance in the current understanding of the interspecific variability to ammonium nutrition, we investigated the performance of the three annual species of *Brachypodium* genus: *B. distachyon*, *B. stacei*, and *B. hybridum,* focusing on their differential responses to ammonium and nitrate nutrition. *B. stacei* appeared as a tolerant species, with equal growth regardless of the N source, and *B. distachyon* as the most sensitive, while *B. hybridum* showed an intermediate phenotype. Metabolomic analysis highlighted critical differences in N metabolism, where *B. stacei* and *B. hybridum* exhibited more robust N assimilation in terms of protein content. In addition, several metabolic pathways were found associated with ammonium nutrition. Notably, flavonoid biosynthesis and tricarboxylic acid cycle pathways together with ethylene precursors and iron homeostasis-related compounds contributed to explain species-specific responses to ammonium nutrition. Altogether, these findings pinpoint potential strategies for improving N utilization and ammonium stress tolerance in cereals.

1. Introduction

Nitrogen (N) use efficiency (NUE) in crops, defined as the amount of applied N recovered from harvest, is estimated around 40 %, with the remaining 60 % contributing to environmental pollution (Good and Beatty, 2011). This is because nitrate (NO_3^-), the principal N form in agricultural soils, is prone to leaching and contaminates water resources. In addition, soil N, notably through NO_3^- denitrification, can be converted to N gases such as nitrous oxide (N_2O), a powerful greenhouse gas that contributes to global warming. The other main source of inorganic N is ammonium (NH_4^+), which represents a better option to mitigate N contamination and to improve NUE due to its longer availability in soil and its rapid assimilation into biomolecules (Marino and Moran, 2019; Subbarao and Searchinger, 2021). In fact, over the last decades, the use of nitrification inhibitors combined with NH_4^+ nutrition has attracted attention due to the environmental advantages of delaying the conversion of NH_4^+ to NO_3^- (Rodríguez et al., 2024). In this sense, the Intergovernmental Panel on Climate Change (IPCC) recommends the use of urease and nitrification inhibitors as a mitigation option for agricultural N losses (IPCC, 2014). However, despite the environmental benefits that NH_4^+-based fertilization has compared to NO_3^--based nutrition, a high concentration of NH_4^+ in soils can provoke stress in most crops. Much research has been conducted focused on understanding the causes and molecular mechanisms associated with NH_4^+ stress and, it is now accepted that NH_4^+ toxicity involves, among others, pH disequilibrium, hormone imbalance, energy trade-off and metabolic alterations (Liu and von Wirén, 2017; Coleto et al., 2023; Xiao et al., 2023).

Regarding the metabolic alterations, the plant experiences a significant reprogramming of carbon (C) and N metabolism towards amino acid synthesis. Indeed, the adjustment of primary metabolism is essential for the natural variation of NH_4^+ tolerance in *Brachypodium distachyon* (De la Peña et al., 2024). Further understanding of plant metabolism under NH_4^+ stress may lead to breeding strategies to enhance crop performance under NH_4^+ nutrition. In this context, non-targeted

* Corresponding authors.
E-mail addresses: daniel.marino@ehu.eus (D. Marino), mariabegona.gonzalez@ehu.eus (M.B. González-Moro).
[1] Colombian Sugar Cane Research Center (CENICAÑA), Cali, Colombia.

https://doi.org/10.1016/j.plantsci.2025.112684
Received 26 February 2025; Received in revised form 23 July 2025; Accepted 25 July 2025
Available online 29 July 2025

metabolomics may provide a more comprehensive description of the complex metabolic networks for understanding NUE.

Brachypodium genus belongs to the Pooideae subfamily and thus, is closely related to economically relevant forage grasses and cereals, such as oat, rye, wheat and barley. Within this genus, the species *Brachypodium distachyon* has progressively come to the forefront for research on grasses as a model organism thank to its small genome, self-fertility, small size and short life cycle (Scholthof et al., 2018). For more than a century, *B. distachyon* was considered as the single annual species of *Brachypodium* genus. Importantly, Catalán et al. (2012) reported that what had been considered as a single species actually comprised three distinct species, and subsequently named the two novel species as *Brachypodium stacei* and *Brachypodium hybridum*. These three species consist of two diploid parents with different chromosome base number: *B. distachyon* (x = 5; 2 n = 10) and *B. stacei* (x = 10; 2 n = 20), and their derived allotetraploid hybrid *B. hybridum* (x = 5 +10; 2 n = 30). All three species are native from the Mediterranean region but *B. distachyon* is typically found in cooler, wetter and higher-altitude environment, *B. stacei* in drier, warmer and lower-altitude areas and *B. hybridum* in both ancestral environments and intermediate conditions (Martínez et al., 2018; Takahagi et al., 2018). Notably, *B. hybridum* has spread worldwide, surpassing the range of either of its diploid progenitors, thus suggesting a higher adaptability to different environments (Scholthof et al., 2018). In addition, *B. hybridum* has advantages regarding resistance to external stresses. For instance, *B. hybridum* showed a transgressive expression pattern in leaf phytohormone content compared with its parental species, which confers significantly greater tolerance response to drought (Martínez et al., 2018).

Most studies on N nutrition in *Brachypodium* have focused on *B. distachyon*, given its predominant role as model species (Barhoumi, 2017; David et al., 2019; De la Peña et al., 2019; Wang et al., 2019). For instance, in De la Peña et al. (2019), we reported that the *B. distachyon* Bd21 reference accession responded to NH_4^+ nutrition alike other cereals, such as wheat. Similarly, David et al. (2019), focusing on NO_3^- uptake, also validated the suitability of *B. distachyon* as a tool to decipher cereal N nutrition. In the present work, we aimed to compare the performance of the three annual *Brachypodium* species (*B. distachyon*, *B. stacei* and their natural hybrid *B. hybridum*) when grown under NH_4^+ or NO_3^- nutrition. For this characterization we conducted a metabolomic study combining non-targeted and targeted approaches, with a particular emphasis on metabolic traits related to C and N metabolism, because of its importance for NH_4^+ stress tolerance (González-Moro et al., 2021).

2. Materials and methods

2.1. Plant growth conditions

Brachypodium distachyon Bd21, *B. stacei* ABR114 and *B. hybridum* ABR113 were the three genotypes used in this work. Following the methodology described by Tyler et al. (2016), seeds were peeled by removing the lemma, washed in a solution containing 15 % bleach plus 0.1 % Triton-X 100 for 4 min and thoroughly rinsed with sterile deionized water. To synchronize germination, seeds were placed in Petri dishes on damp paper towels and stratified in the dark at 4°C for 7 days. Afterwards, the plates were covered and incubated in the dark in a growing chamber for 3 days. Germinated seeds were then sowed in trays filled with perlite:vermiculite (1:1, v:v) and misted with deionized water. After 7 days seedlings with a uniform appearance were transferred to hydroponic tanks (12 plants per tank) filled with 4.5 L of nutrient solution containing 2.5 mM N, provided as either NO_3^- or NH_4^+. Three tanks (experimental units) were established per species and condition. The nutrient solution contained 1.15 mM K_2HPO_4, 0.85 mM $MgSO_4$, 0.7 mM $CaSO_4$, 2.68 mM KCl, 0.5 mM $CaCO_3$, 0.07 mM NaFeEDTA, 16.5 μM Na_2MoO_4, 3.7 μM $FeCl_3$, 3.5 μM $ZnSO_4$, 16.2 μM H_3BO_3, 0.47 μM $MnSO_4$, 0.12 μM $CuSO_4$, 0.21 μM $AlCl_3$, 0.126 μM $NiCl_2$ and 0.06 μM KI (pH 6.8). The N source was $(NH_4)_2SO_4$ for NH_4^+-fed plants and $Ca(NO_3)_2$ for NO_3^--fed ones. To compare both N sources, NO_3-fed plants were supplied with $CaSO_4$ to balance the sulfur supplied with the NH_4^+. Plants were grown under hydroponic conditions for 19 days. Environmental conditions in the growth chamber were set to a light period of 14 h (23 °C, 60 % relative humidity, light intensity 350 μmol m^{-2} s^{-1}) and a dark period of 10 h (18 °C, 70 % relative humidity). The nutrient solution was replaced every 4 days, where the stability of pH in the nutrient solution was confirmed. Shoots and roots were separated and weighed. Plants grown within the same tank were pooled, immediately frozen in liquid nitrogen, homogenized in a Tissue Lyser (Retsch MM 400) and stored at −80 °C until use.

2.2. Enzyme activities

For enzyme activities approximately 20 mg of frozen shoot or root tissue powder was homogenized by vigorous mixing in 500 μl of extraction buffer composed of 20 % (v/v) glycerol, 0.25 % (w/v) bovine serum albumin, 1 % Triton X-100 (v/v), 50 mM HEPES–KOH (pH 7.5), 10 mM $MgCl_2$, 1 mM EDTA, 1 mM EGTA, 1 mM aminocaproic acid, 1 mM benzamidine, 20 μM leupeptin. 0.5 mM dithiothreitol, 1 mM phenylmethylsulfonylfluoride and 10 % polyvinylpolypyrrolidone (w/v) (Gibon et al., 2004). Assays to measure glutamate dehydrogenase (GDH), malate dehydrogenase (MDH), NADP-dependent isocitrate dehydrogenase (ICDH), phosphoenolpyruvate carboxylase (PEPC), pyruvate kinase (PK) and citrate synthase (CS) activity were performed by spectrophotometric methods using a 96-well microplate reader as described in Gibon et al. (2004). The evolution of NAD(P)H was monitored at 340 nm after incubation at 25°C. The activity of GDH was assessed at 570 nm via a cycling reaction involving the reduction of 3-(4, 5-dimethylthiazol-2-yl)-2,5-diphenyl tetrazolium bromide in the presence of alcohol dehydrogenase and phenazine ethosulfate to quantify NAD^+.

2.3. Targeted metabolite quantification

The extraction for chlorophyll, NH_4^+, NO_3^- and the metabolites shown in Figs. 2 and 3 was performed as described in De la Peña et al. (2024). Briefly, 20 mg of frozen tissue powder (shoot or root) was extracted in 250 μL of 80 % ethanol, 10 mM HEPES/KOH (pH 6), incubated for 20 min at 80 °C, centrifuged at 14,000 *g* for 5 min at 4°C and the supernatant was recovered. This process was repeated with 150 μL of 80 % ethanol, 10 mM HEPES/KOH (pH 6) and 250 μL of 50 % ethanol in 10 mM HEPES/KOH (pH 6). The three supernatants were pooled and the pellet resuspended in 400 μL of 0.1 M NaOH.

Chlorophyll quantification was determined by empirical adaptation of the formula of Arnon (1949) to the microplate reader. NH_4^+ content was quantified as described in Sarasketa et al. (2014). Total content of free amino acids was assayed as described by Bantan-Polak et al. (2001). Glutamate, soluble sugars (glucose, fructose, sucrose), malate, citrate, proteins, starch and glutathione were quantified as described in De la Peña et al. (2024).

2.4. Non-targeted metabolomic analysis through LC-MS profiling

For non-targeted metabolomic analysis, 100 mg of frozen tissue (shoot or root) powder was extracted in 0.5 mL of methanol:water:formic acid (80:20:0.1, v/v/v) using a Retsch mixer mill for 4 min at 30 Hz. The samples were then centrifuged at 14000 *g* for 3 min and the supernatant was placed in an HPLC glass vial fitted with a conical insert.

Metabolite analysis was performed with a UPLC-QTOF-MS instrument equipped with an electrospray ionization (ESI) source (Waters Synapt G2). An aliquot of 2.5 μL of methanolic extract was injected into an Acquity UPLC (Waters) and separated on an ACQUITY UPLC® BEH C18 (50 ×2.1 mm, 1.7 μm) column at 40 °C. Mobile phase A was 0.05 % formic acid in water (v/v), and mobile phase B was 0.05 % formic

acid–acetonitrile (v/v). The gradient was as follows: 0 min, 2 % B; 3 min, 35 % B; 6 min, 100 % B; 7.5 min, 100 % B; 7.6 min, 2 % B. The flow rate was 0.6 mL/min, and the target sample temperature was 20 °C. Detection was performed in negative and positive ion modes in the *m/z* range 80–1200 with a total scan time of 0.2 s. The acquisition was performed in data-independent mode (DIA) with the mass spectrometer switching alternatively from low (4 eV, 0.1 s scan time) to high (10–30 eV, 0.1 s scan time) collision energies. ESI conditions were as follows: capillary voltage + 2.8/-2.0 kV, cone voltage 25 V, source temperature 120 °C, desolvation temperature 400 °C, cone gas flow 20 L/h, and desolvation gas flow 900 L/h. For internal calibration, a leucine–enkephalin solution (Sigma–Aldrich, Steinheim, Germany) at 0.5 μg/mL was infused through the Lock Spray™ probe at a flow rate of 15 μL/min as a lockmass. Acquired data were processed using Waters MassLynx v 4.1 software.

The data obtained after analysis of the extracts by UPLC-TOF-MS in negative and positive mode of ionization were converted from the vendor file format (*.raw from Waters) into the common file format of Reifycs Inc. (Analysis Base File format *.abf) using the freely available Reifycs 211 ABF converter (http://www.reifycs.com/AbfConverter/index.html). The sorted data was processed by MS-DIAL software (v. 4.20) for feature detection, chromatogram construction, chromatogram deconvolution, isotopic peak grouping, chromatogram alignment, peak filtering, and gap filling. The parameters used for data processing are described in Table S1. Since the quality control (QC) samples did not consist of a mixture of all samples, but of similar samples from one shoot replicate of NH_4^+ stress in *B. distachyon*, a randomly chosen sample was selected as a reference file to build up the alignment table. MS2Dec algorithm in MS-DIAL was applied for spectra deconvolution in the respective precursor ion range. Here peak area, also referred as peak intensity, is related to sample concentration.

2.5. Statistical analysis

Biomass, individually determined metabolites and enzyme activities were analyzed using a two-way ANOVA. For non-targeted metabolomics, principal component analysis (PCA) was performed on shoot and root metabolomics data using the "FactoMineR" and "factoextra" packages in R. Metabolic pathway analysis was performed using the mummichog algorithm in MetaboAnalyst 6.0, with analysis parameters set to ±5 ppm mass tolerance, retention time matching, standard LC-MS adduct settings, and unadjusted two-way ANOVA p-values for treatment or interactions effects. This analysis was conducted separately for shoot and root tissues, using the *Triticum aestivum* metabolome reference library, mapped 481 of 2709 initial mass features to putative metabolites. Representative metabolites were summarized by selecting features with the lowest ANOVA FDR values when multiple features mapped to the same metabolite. Additionally, student's t-tests were used for pairwise analysis to determine the significance of the N source within a given species. Finally, for physiological measurements, targeted metabolite determination and enzyme activities we also conducted one-way ANOVA analysis followed by Duncan's post-hoc test ($P < 0.05$) as shown in Table S2.

3. Results and discussion

3.1. B. stacei and B. hybridum show enhanced tolerance to ammonium stress

Plant growth is the most integrative indicator of plant performance and, surely, the best marker of NH_4^+ stress. We compared the biomass accumulation of three related *Brachypodium* species under the exclusive supply of NH_4^+ with that of plants grown with an exclusive supply of NO_3^- as control condition. The results revealed a species effect, with *B. hybridum* exhibiting superior growth compared to both *B. stacei* and *B. distachyon*, regardless of the N source (Fig. 1A). Previous studies reported superior growth for both *B. stacei* and *B. hybridum* compared to

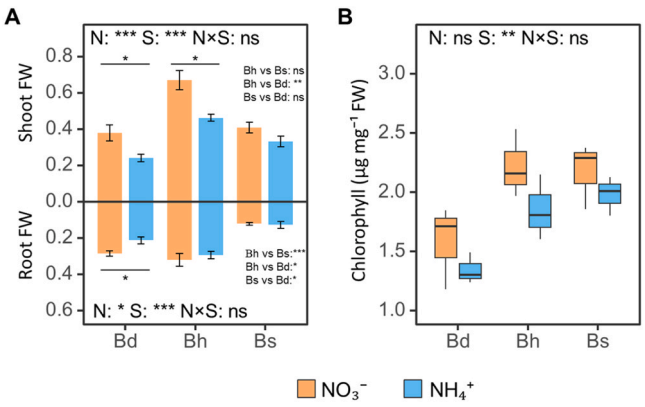

Fig. 1. Fresh weight (g FW plant^{-1}) (A) and content of chlorophyll (B) of *Brachypodium distachyon* (Bd), *B. hybridum* (Bh) and *B. stacei* (Bs) under ammonium and nitrate nutrition. Statistical significance levels for the main effects and interactions between nitrogen source (N) and Species (S) are denoted by asterisks (* $P < 0.05$, ** $P < 0.01$, and *** $P < 0.001$), and non-significant results are labeled as (ns). In cases where the species factor was significant but not the interaction, Tukey's post-hoc comparisons was used to display significant differences among the species. Asterisks between bars indicate biomass differences between nitrogen sources within a species by the student's t tests.

B. distachyon with *B. hybridum* showing higher values for several morphometric traits (e.g. Catalán et al., 2012; López-Álvarez et al., 2017). In our work, superior growth was not observed for *B. stacei*, which may be attributed to the still early developmental stage of the plant or to the experimental methodology (hydroponics respect to soil/substrate). As expected, NH_4^+ supply reduced growth for both *B. distachyon* and B. *hybridum*, while the latter was able to maintain root growth. In contrast, the growth of *B. stacei* was similar under both N sources (Fig. 1A). Chlorophyll content is another common marker for determining the degree of stress suffered by plants when growing with NH_4^+. Indeed, under a mild NH_4^+ stress plants often display increased chlorophyll content, while chlorosis appears when the stress becomes severe (Sánchez-Zabala et al., 2015). In our study, the chlorophyll content tended to be lower under NH_4^+ nutrition for all species, but not significant N source effect was observed (Fig. 1B).

3.2. Primary N and C metabolism adapts to ammonium stress in Brachypodium genus

Ammonium-based nutrition entails the accumulation of free NH_4^+ in tissues leading to the induction of N assimilation. Whether the increase in N assimilation benefits plant performance remains unclear. On the one hand, enhancing N assimilation scavenges the excess of NH_4^+. On the other hand, an excessive N assimilation may represent an energy trade-off and contributes to cell acidification, as the incorporation of NH_4^+ to glutamate releases one proton (Hachiya et al., 2021). In general, increasing NH_4^+ assimilation in the root seems beneficial; for instance, the Arabidopsis mutant for the cytosolic GLN1;2 glutamine synthetase (GS) isoform is sensitive to NH_4^+ stress (Guan et al., 2016). Conversely, a higher increment of N assimilation in the aerial part appears as detrimental (Poucet et al., 2021). For instance, an Arabidopsis mutant lacking the plastidic GS (GLN2) showed enhanced tolerance to NH_4^+ stress (Hachiya et al., 2021).

In the aerial part, NH_4^+ and amino acid content increased under NH_4^+ nutrition in a similar manner for the three species, while protein content remained unchanged (Fig. 2). In roots, NH_4^+ accumulation showed significant NxS interaction, with the magnitude of NH_4^+ accumulation between both N treatments following the pattern *B. stacei* > *B. hybridum* > *B. distachyon*. The huge preferential NH_4^+ accumulation in the root can been interpreted as a physiological barrier to prevent deleterious NH_4^+

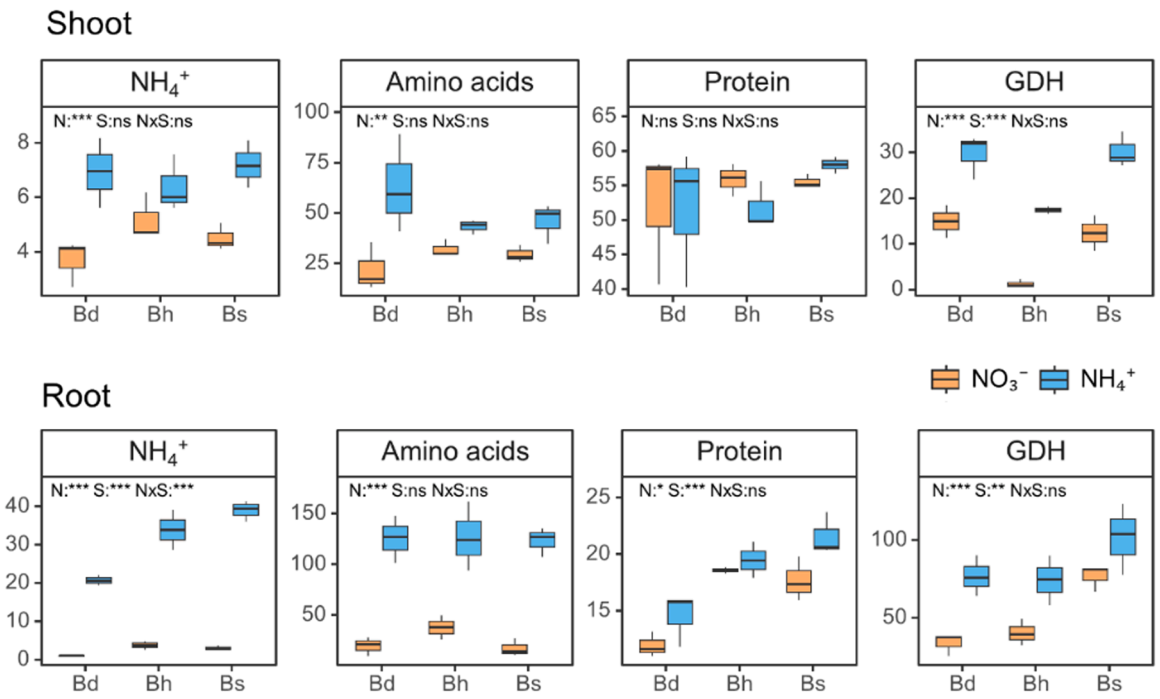

Fig. 2. Nitrogen assimilation-related traits in leaf and root tissues of *B. distachyon* (Bd), *B. hybridum* (Bh), and *B. stacei* (Bs) under NH_4^+ or NO_3^- nutrition. Measurements include total amino acids content (μmol g^{-1} FW), GDH activity (μmol NADH g^{-1} FW h^{-1}), NH_4^+ content (μmol g^{-1} FW) and protein content (mg BSA g^{-1} FW). Two-way ANOVA results show significance levels for nitrogen source (N), species (S), and their interaction (N × S). *p ≤ 0.05, **p ≤ 0.01, ***p ≤ 0.001.

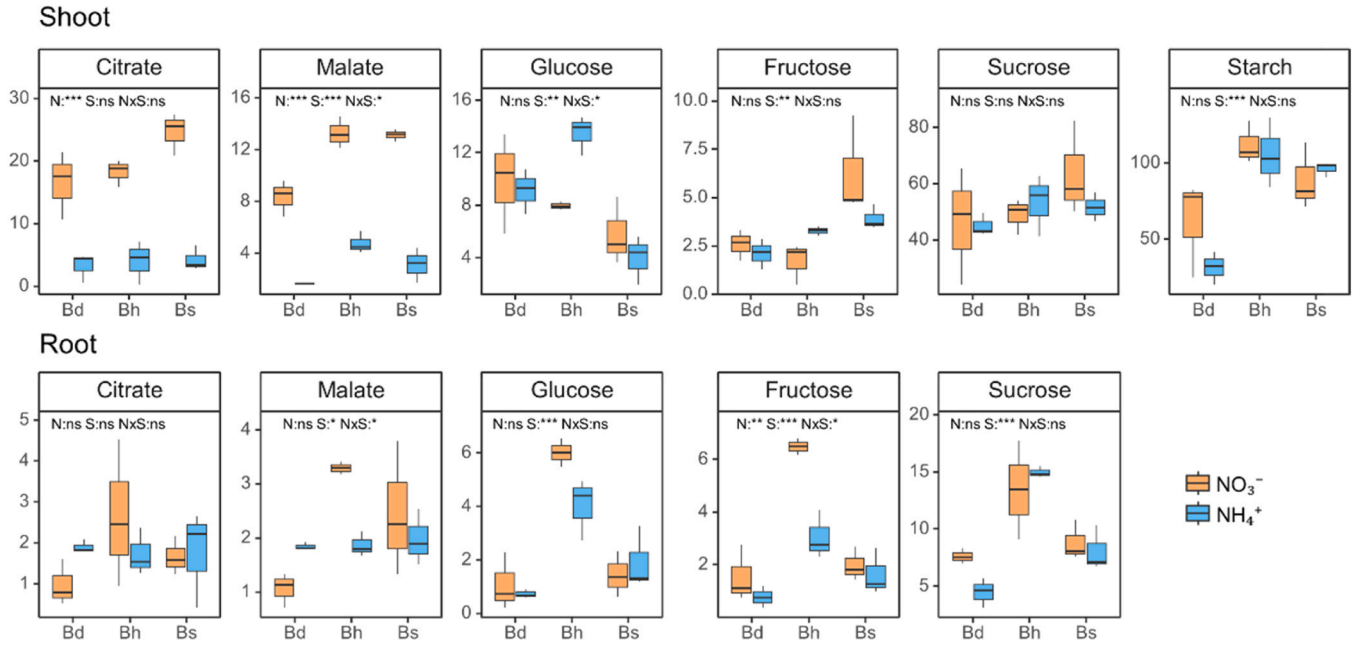

Fig. 3. Carbon-related metabolites in leaf and root tissues of *B. distachyon* (Bd), *B. hybridum* (Bh), and *B. stacei* (Bs) under NH_4^+ or NO_3^- nutrition. Measurements include citrate (nmol mg^{-1} FW), malate (nmol mg^{-1} FW), fructose (eq μmol Gluc g^{-1} FW), glucose (eq μmol Gluc g^{-1} FW), starch (eq μmol Gluc g^{-1} FW), and sucrose (eq μmol Gluc g^{-1} FW). Two-way ANOVA results show significance levels for nitrogen source (N), species (S), and their interaction (N × S). *p ≤ 0.05, **p ≤ 0.01, ***p ≤ 0.001.

accumulation in the aerial part (González-Moro et al., 2021). This pattern of NH_4^+ accumulation aligns with the relative root biomass tolerance for each species (Fig. 1A). Consistently, amino acid and protein accumulation was also markedly higher in the root respect to the shoot (Fig. 2), supporting that the primary metabolic adjustment to NH_4^+ nutrition took place in the root. However, no clear correlation was observed between total N content (Figure S1) and the ammonium tolerance degree (Fig. 1). GDH activity, a well-known metabolic marker of NH_4^+ nutrition (Patterson et al., 2010; González-Moro et al., 2021), was also higher in roots and was induced by NH_4^+ nutrition in both organs for the three species (Fig. 2). Indeed, in *B. distachyon* GDH2 was suggested as one of the metabolic determinants of NH_4^+ tolerance (De la Peña et al., 2024). It is still controversial whether GDH works in aminating 2-oxoglutarate or deaminating glutamate or whether its function

is species-dependent (Dubois et al., 2003; Vega-Mas et al., 2019). In our study, GDH did not show a significant NxS interaction; however, in the root, its activity was higher for *B. stacei* compared to both relatives, suggesting it might contribute to the better tolerance of this species towards NH_4^+ nutrition.

The synthesis of amino acids requires C skeletons, a demand that becomes particularly intense under NH_4^+ nutrition. In this scenario, the tricarboxylic acid (TCA) cycle adjusts its activity to operate in an open-flux mode, diverting C skeletons -mainly 2-oxoglutarate, but also oxaloacetate- for NH_4^+ assimilation (González-Moro et al., 2021). In fact, the depletion of organic acids and the induction of TCA-associated enzymes activity are common responses to NH_4^+ stress, as reported in many species including *B. distachyon* (De la Peña et al., 2019). To evaluate potential interspecies difference regarding C metabolism, we determined the content of main soluble sugars (glucose, fructose and sucrose), the two most abundant TCA cycle organic acids (malate and citrate) and starch (Fig. 3). In shoot, citrate and malate content was significantly lower under NH_4^+ nutrition. In roots, the organic acid content was much lower than in leaves and the N source had a different behavior between species. Notably, citrate and malate accumulated upon NH_4^+ stress in *B. distachyon*, while they decreased in *B. hybridum*, with no difference observed for the more tolerant *B. stacei*. Organic acid accumulation in *B. distachyon,* considering it was the only species in which root biomass decreased, suggests impaired use of C resources for N assimilation. For sugars, no interaction effect (NxS) was observed; however, *B. hybridum* showed a higher soluble sugars content in roots and starch in the shoot (Fig. 3), suggesting a superior photosynthetic performance and a more efficient C allocation that could be associated with the superior growth of this species. In agreement, *B. hybridum* presented a higher shoot C/N balance and higher root C content respect of the two other species (Figure S1).

3.3. Non-targeted metabolomics underlines pathways associated with ammonium tolerance in the Brachypodium genus

To further understand the species-dependent metabolic adaptation to NH_4^+ nutrition, we looked for metabolites and metabolic pathways associated to the response of the *Brachypodium* genus to the N source using non-targeted metabolomics. We conducted this analysis in positive and negative ionization modes and detected a total of 2709 metabolic features in all samples (Table S3). As autotrophic and heterotrophic organs, the metabolism of leaves and roots is different. Therefore, to prevent the organ effect from masking impact effect of the species and the N source, we performed exploratory analyses separately for each organ. Principal component analysis (PCA) revealed a hierarchical organization of the factors influencing the metabolic variation (Fig. 4). Both organs exhibited a similar pattern of species and condition distribution, with the PCA explaining 52.8 % of the total variation for shoot and 29.5 % for root. The primary source of variance was the species, captured by PC1 (34.9 % for shoot and 17 % for root), with *B. distachyon* showing the greatest divergence, while *B. hybridum* displayed an intermediate phenotype more closely aligned with *B. stacei* (Fig. 4). The N source contributed the second level of variation (PC2, 17.9 % for shoot and 12.5 % for root), with a clear separation observed in both organs, as indicated by the distinctive clustering of NH_4^+ and NO_3^- treatments (Fig. 4).

To place the metabolomics changes into the biological context, we analyzed the dataset considering their statistical significance (p-value < 0.05; Table S3) with respect to the N source effect using the MetaboAnalyst 6.0 platform (Pang et al., 2024). To achieve this, we used the

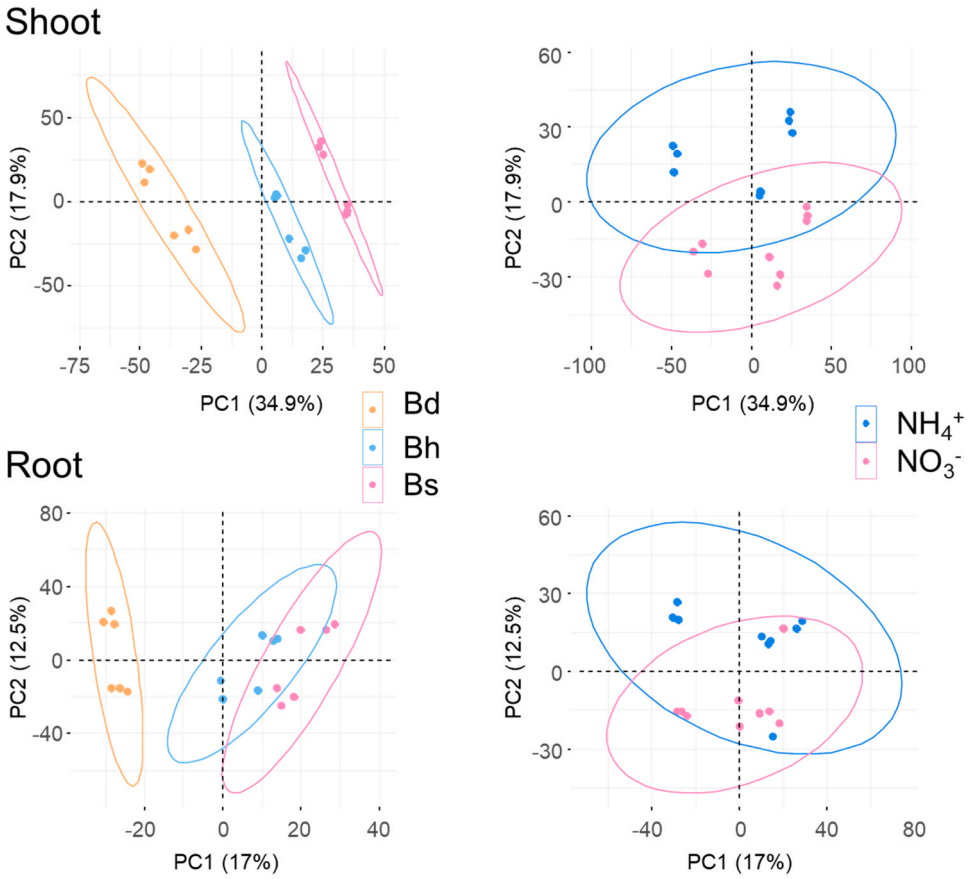

Fig. 4. Principal Component Analysis (PCA) of non-targeted metabolomic data separated by plant organs (shoot and root) in *Brachypodium* species under different nitrogen sources. Left panels show the distribution of three *Brachypodium* species: Bd (*B. distachyon,* orange), Bh (*B. hybridum*, blue), and Bs (*B. stacei*, pink). Right panels display the separation by nitrogen source treatments: NH_4^+ (blue) and NO_3^- (pink).

pathway library for *Triticum aestivum* (bread wheat) and the mummichog algorithm (Figs. 5A and 5B). As recommended by MetaboAnalyst 6.0, the complete dataset was employed to establish an accurate null model for background estimation. Mummichog algorithm is particularly valuable for analyzing unannotated metabolic features, as it assigns putative annotations and identifies significant pathways without requiring confident metabolite identification (Li et al., 2013). The underlying principle is that while individual metabolite annotations may be uncertain, pathway-level enrichment remains meaningful due to the non-random distribution of true metabolites within biochemical pathways.

In shoots, the metabolic pathway enrichment analysis focused on the N source effect identified three significantly enriched pathways (Fisher's exact test with FDR correction): "citrate cycle (TCA cycle)" showed the highest enrichment (FDR = 8.29×10^{-4}), followed by "glyoxylate and dicarboxylate metabolism" (FDR = 2.70×10^{-3}), and "carbon fixation in photosynthetic organisms" (FDR = 1.31×10^{-2}) (Fig. 5A). The metabolites associated to these pathways are shown in Table S4. The fact that the three pathways are associated to primary C metabolism, highlights the importance of energy production and C supply for N assimilation, as already arouse by organic acid and sugar levels (Fig. 3). The enrichment of the TCA cycle, associated to the lower content of aconitate, fumarate, succinate, pyruvate, oxaloacetate, oxoglutarate and malate in the three species, along with the accumulation of Asp, Glu and Gln under NH_4^+ nutrition, is surely responsible for the higher total amino acid level (Fig. 2). The glyoxylate pathway, is closely intertwined with the TCA pathway, as it bypasses the oxidative decarboxylation steps of this cycle, converting isocitrate to succinate and glyoxylate via the activity of isocitrate lyase. In a second step, malate synthase renders malate from glyoxylate and acetyl-CoA, without CO_2 loss and thus, glyoxylate pathway conserves C skeleton production in form of malate or C4 acids (Eastmond and Graham, 2001). In the context of NH_4^+ nutrition, the glyoxylate pathway may have an anaplerotic function, replenishing intermediates of the TCA cycle (Eprintsev et al., 2015).

In the root, the enrichment pathway analysis focused on the effect of N source effect did not identify any pathway meeting the stringent significance threshold (FDR < 0.05); however, two major pathways approached significance (FDR < 0.1): "cysteine and methionine metabolism" (FDR = 7.5×10^{-2}) and "glyoxylate and dicarboxylate metabolism" (FDR = 7.53×10^{-2}) (Fig. 5B). The latter associated with several organic acids and amino acids, a pathway also retrieved in shoots. Detailed metabolite profiling revealed distinct patterns between NH_4^+ and NO_3^- nutrition across these pathways (Table S4). Considering the highlighted importance of the TCA cycle, we complemented the metabolite profiling by determining the activity of enzymes associated to TCA cycle (ICDH, MDH, PEPC, PK, CS). The N source significantly affected CS activity both in shoot and root (Fig. 6). PEPC activity was also induced in the root upon NH_4^+ nutrition; notably, in *B. hybridum* that showed an overall higher root PEPC activity. Indeed, RNAi sorghum lines silenced for the root PEPC isoform (*SbPPC3*) presented enhanced sensitivity to NH_4^+ stress and a higher NH_4^+ accumulation in the root, thus providing a genetic evidence of the importance of TCA cycle under ammonium nutrition (Marín-Peña et al., 2024). *B. hybridum* also showed higher PK activity in the root, an enzyme responsible for the last step of glycolysis, which was probably induced by its higher root sugar availability (Fig. 3). This further suggests a more active C metabolism, which would contribute to the more vigorous growth of this species. In the shoot, the more tolerant *B. stacei* presented the highest CS and PK activities, which may be facilitating the use of C resources in this species.

3.4. Non-targeted metabolomics depicts significant metabolites associated with the differential Brachypodium responses

In order to identify potential metabolites associated with the varying response observed among the three species, we paid special attention to the metabolic features significantly affected by the NxS interaction (p-value < 0.05; Table S3). In the aerial part, pathway enrichment analysis revealed significant enrichment of two flavonoid-related pathways: "flavone and flavonol biosynthesis" and "flavonoid biosynthesis" (Fig. 7A). Indeed, several flavonoids associated to these pathways exhibited significant NxS interaction effect (FDR < 0.05) (Table 1). For instance, the accumulation of flavonoids, such as the tentatively annotated kaempferol and isoquercitrin, was especially relevant in *B. stacei* under NH_4^+ nutrition compared to NO_3^- nutrition. Several other flavonoids, including putative biochanin, daidzein, and rutin, also displayed species-specific responses to the N source, with notable different accumulation patterns across the three *Brachypodium* species.

Flavonoids are specialized metabolites with many different biological functions. One of their best-recognized properties is their ability to function as antioxidants through direct scavenging or reactive oxygen species (ROS) or via its metal-chelating activity. ROS overproduction has been often reported in plants exposed to NH_4^+ stress. Indeed, altering antioxidant systems has been shown to affect the tolerance of plants to NH_4^+ stress (Liu and von Wirén, 2017; Xiao et al.,2023). The origin of NH_4^+-dependent ROS overproduction is not completely understood but it has been linked to, among others, increased mitochondrial electron transport chain activity (Rasmusson et al., 2020) and the Fenton reaction because of reactive iron (Fe) accumulation in the root (Liu et al., 2022a). In this sense, it is noteworthy that *B. stacei* was the only species that displayed a significant accumulation of flavonoids, a response not

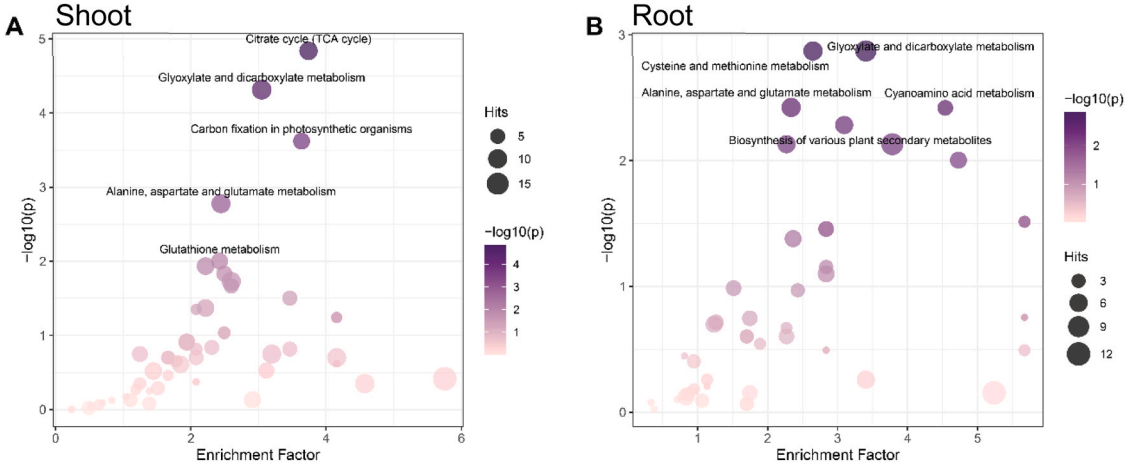

Fig. 5. Metabolic pathway enrichment analysis using the mummichog algorithm in *Brachypodium* shoot (A) and root (B) for the metabolites showing significant nitrogen source effect (two-way ANOVA).

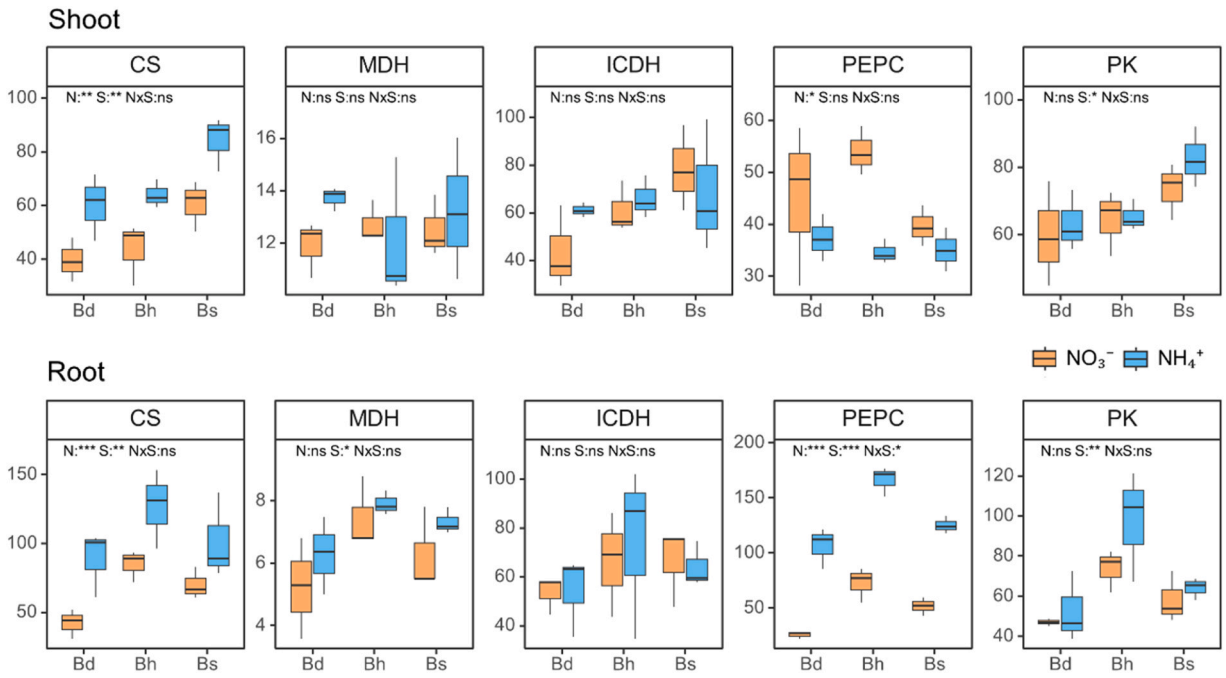

Fig. 6. TCA-associated enzyme activities in *B. distachyon* (Bd), *B. hybridum* (Bh), and *B. stacei* (Bs) under ammonium and nitrate nutrition in both shoot and root. Measurements include citrate synthase (CS; μmol NADH g^{-1} FW h^{-1}), malate dehydrogenase (MDH; mmol NADH g^{-1} FW h^{-1}), isocitrate dehydrogenase (ICDH; μmol NADPH g^{-1} FW h^{-1}), phosphoenolpyruvate carboxylase (PEPC; μmol NADH g^{-1} FW h^{-1}), and pyruvate kinase (PK; μmol NADH g^{-1} FW h^{-1}). Asterisks indicate the level of significance of the ANOVA due to the factors nitrogen source (N), species (S), and the interaction between nitrogen source and species (N × S). *: $p \leq 0.05$; **: $p \leq 0.01$; ***: $p \leq 0.001$.

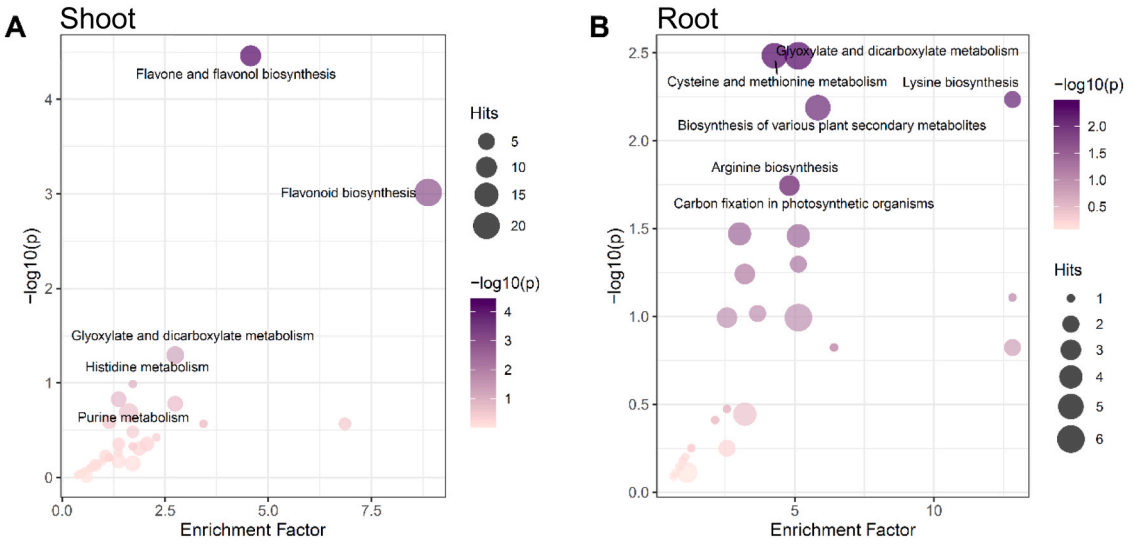

Fig. 7. Metabolic pathway enrichment analysis using the mummichog algorithm in Brachypodium shoot (A) and root (B) for the metabolites showing significant nitrogen source x species (NxS) interaction effect (two-way ANOVA).

observed in *B. distachyon* or *B. hybridum* (Table 2). Therefore, we can hypothesize that flavonoids may contribute to the observed NH_4^+ tolerance of *B. stacei* (Fig. 1). As a marker of plant redox status we determined the total content of reduced (GSH) and oxidized glutathione (GSSG) and calculated their ratio (GSH/GSSG) (Figure S2). The high variability among replicates hindered the statistical significance but the general trends observed do not support the involvement of glutathione in the species-effect on ammonium tolerance.

In roots, the analysis focused on the significant NxS interaction revealed several enriched pathways (FDR ≤ 0.05) (Fig. 7B) associated with 13 metabolic features presented in Table 2. Among these, primary C and N metabolites also showed significant NxS interaction. Glu was accumulated in *B. stacei* and *B. hybridum*, while it decreased in *B. distachyon*. Additionally, the content of the carboxylic acids tentatively annotated as citrate, oxoglutarate and oxaloacetate was lower in the root of *B. hybridum* and *B. stacei* while it increased in *B. distachyon*. These results are consistent with the targeted metabolites determination (Fig. 3) and suggest a higher N assimilation capacity for *B. hybridum* and *B. stacei* that may contribute to their higher NH_4^+ tolerance compared to *B. distachyon* as previously discussed.

Interestingly, several key compounds were associated to root "cysteine and methionine metabolism" pathway. These metabolites

Table 1
Metabolic features with their tentative annotation from leaf pathway enrichment analysis of the N source × species (NxS) interaction.

Pathway	Class	Tentative annotation	Query Mass	Matched Form	RT	*B. distachyon*		*B. hybridum*		*B. stacei*	
						Ammonium	Nitrate	Ammonium	Nitrate	Ammonium	Nitrate
FB	F	(-)-Epiafzelechin[a]	297.074	M+Na[1 +]	1.65	3.2 ± 0.0	3.18 ± 0.0	3.2 ± 0.0**	3.1 ± 0.0	3.2 ± 0.0**	3.05 ± 0.0
FB	F	(2 R)−2-(3.4-Dihydroxyphenyl)−3.5.7-trihydroxy−2.3-dihydrochromen−4-one[b]	285.04	M-H2O-H[-]	1.655	3.4 ± 0.0	3.40 ± 0.0	3.6 ± 0.0	3.6 ± 0.0	3.6 ± 0.0**	3.46 ± 0.0
FB	O	3-O-p-Coumaroylquinic acid	337.093	M-H[-]	1.425	3.2 ± 0.0*	3.44 ± 0.0	2.8 ± 0.0	2.7 ± 0.0	2.8 ± 0.0*	2.66 ± 0.0
FB	F	Aromadendrin[c]	308.032	M+Na-2H[-]	2.283	0.7 ± 0.1**	1.35 ± 0.1	3.4 ± 0.0	3.4 ± 0.0	3.5 ± 0.0*	3.45 ± 0.0
FF	F	Astragalin	431.098	M-H2O+H [1 +]	1.641	3.3 ± 0.0*	3.09 ± 0.0	3.2 ± 0.0	3.2 ± 0.0	3.3 ± 0.0*	3.11 ± 0.0
FF	F	Biorobin	575.14	M-H2O-H[-]	2.208	4.1 ± 0.0*	4.01 ± 0.0	3.7 ± 0.0**	3.7 ± 0.0	3.9 ± 0.0**	3.52 ± 0.0
FB	L	Butein[d]	295.059	M+Na[1 +]	1.643	3.7 ± 0.0*	3.66 ± 0.0	3.2 ± 0.0	3.2 ± 0.0	3.1 ± 0.0*	2.94 ± 0.0
FB	C	Dattelic acid	335.078	M-H[-]	1.399	2.4 ± 0.0	2.40 ± 0.1	3.2 ± 0.2	2.6 ± 0.1	2.7 ± 0.0***	2.33 ± 0.0
FF	F	Isoquercitrin	445.078	M-H2O-H[-]	1.654	3.9 ± 0.0	3.88 ± 0.0	4.1 ± 0.0	4.0 ± 0.0	4.1 ± 0.0***	3.83 ± 0.0
FB. FF	F	Kaempferol	285.04	M-H[-]	1.655	3.4 ± 0.0	3.40 ± 0.0	3.6 ± 0.0	3.6 ± 0.0	3.6 ± 0.0***	3.46 ± 0.0
FB	F	Pentahydroxyflavanone	285.04	M-H2O-H[-]	1.655	3.4 ± 0.0	3.40 ± 0.0	3.6 ± 0.0	3.6 ± 0.0	3.6 ± 0.0**	3.46 ± 0.0
FB	L	Phloretin	297.074	M+Na[1 +]	1.65	3.2 ± 0.0	3.18 ± 0.0	3.2 ± 0.0**	3.1 ± 0.0	3.2 ± 0.0**	3.05 ± 0.0
FF	F	Rutin	565.156	M-HCOOH+H [1 +]	1.645	4.5 ± 0.0*	4.46 ± 0.0	3.9 ± 0.0	3.9 ± 0.0	3.8 ± 0.0**	3.51 ± 0.0
FB	F	trans−3.3′.4′.5.5′.7-Hexahydroxyflavanone	319.045	M-H[-]	1.012	3.3 ± 0.0	3.48 ± 0.1	3.3 ± 0.0*	3.7 ± 0.1	3.8 ± 0.0	3.58 ± 0.1

For pathway, FB means "Flavonoid biosynthesis" and FF "Flavone and flavonol biosynthesis".
For compound class, F means "Flavonoids", O "Organooxygen compounds, L "Linear 1,3-diarylpropanoids", C "Cinnamic acids and derivatives"
In tentative annotation: [a]Also matched to 5-Deoxyleucopelargonidin, afzelechin, and apiforol; [b]Also matched to luteolin; [c]Also matched to eriodictyol, eriodictyol chalcone and fustin; [d]Also matched to butin, chalconaringenin, garbanzol, naringenin and pinobanksin 5-[galactosyl-(1->4)-glucoside]
RT: Retention time in minutes.
Asterisks indicate significant differences between ammonium and nitrate treatments (* $p < 0.05$; ** $p < 0.01$; *** $p < 0.001$).

included 1-aminocyclopropanecarboxylic acid (ACC), which showed higher accumulation in *B. distachyon* upon NH_4^+ nutrition compared to NO_3^- nutrition (Table 2). ACC is the precursor or ethylene. Ethylene synthesis and its related signaling pathways are induced by NH_4^+ (Li et al., 2019; 2022). In fact, ethylene appears as a negative signal in Arabidopsis, as the ethylene-insensitive mutant *ein3* is tolerant to NH_4^+ nutrition (Li et al., 2019). On the contrary, the rice ethylene-insensitive mutant *Oseil1* displayed enhanced sensitivity to NH_4^+ nutrition (Li et al., 2022). In our study, ACC increased exclusively in the root of *B. distachyon* upon NH_4^+ nutrition. Consistently, *B. distachyon* root growth was negatively affected by NH_4^+ nutrition, while the other two species maintained similar root growth under both NH_4^+ or NO_3^- nutrition (Fig. 1A). Therefore, these findings support the idea that ethylene accumulation may be a negative determinant for NH_4^+ sensitivity in *Brachypodium* species.

Furthermore, several compounds related to Fe homeostasis showed distinct patterns, including the phytosiderophores 2-deoxymugineic acid, 3''-deamino-3''-oxonicotianamine, and 3-hydroxymugineic acid, all sharing similar retention times. These metabolites also showed increased accumulation under NH_4^+ nutrition in *B. distachyon* but not in *B. stacei* and *B. hybridum*. This result aligns with a previous study, where we reported that Fe homeostasis was altered in *B. distachyon* upon NH_4^+ nutrition, as evidenced, among others, by the increased abundance of proteins associated with the methionine (Met) cycle and phytosiderophore content (De la Peña et al., 2022). Similarly, recent works highlighted the importance of Fe homeostasis for NH_4^+ tolerance in Arabidopsis (Coleto et al., 2021; Liu et al., 2022a; Liu et al., 2022b; Li et al., 2024). Importantly, both ACC and phytosiderophores are synthesized from S-adenosyl-methionione, an essential plant metabolic intermediate. In addition, the occurrence of O-acetylserine among the 13 metabolites, reinforces the idea that sulfur assimilation participates in NH_4^+-dependent metabolic responses. These results suggest that Met/ethylene and Fe-associated responses may be associated with the differential growth observed among species within the *Brachypodium* genus.

4. Concluding remarks

The three *Brachypodium* annual species showed different degree of NH_4^+ tolerance in terms of growth, where *B. distachyon* was the most sensitive and *B. stacei* the most tolerant. Ammonium nutrition entailed a rearrangement of TCA cycle functioning, suggesting a redirection of carbohydrate flux to support N assimilation. This metabolic strategy was shared by the three species, but differences were observed notably for *B. distachyon,* which displayed the higher sensitivity and presented lower sugar and organic acid accumulation, notably in the shoot. *B. hybridum,* regardless of the N source, exhibited the highest biomass, which might be due to its enhanced C metabolism, as supported by higher sugar and starch content and C-related enzyme activities. In addition, the higher shoot flavonoid levels detected in the more tolerant *B. stacei* and the higher content of root ACC and Fe-associated metabolites content in the more sensitive *B. distachyon* could be associated to the differences observed in NH_4^+ tolerance/sensitivity among these species. Altogether, our work underlines the power of non-target metabolomics and natural variation to unveil mechanisms that can contribute to enhance NH_4^+ tolerance. Future works will help to further

Table 2
Metabolic features with their tentative annotation from root pathway enrichment analysis of the N source × species (NxS) interaction.

Pathway	Class	Tentative annotation	Query Mass	Matched Form	RT	*B. distachyon*		*B. hybridum*		*B. stacei*	
						Ammonium	Nitrate	Ammonium	Nitrate	Ammonium	Nitrate
CM	C	1-Aminocyclopropanecarboxylc acid[a]	100.04	M-H[-]	0.253	3.3 ± 0.0**	1.9 ± 0.1	2.6 ± 0.0	2.4 ± 0.2	2.7 ± 0.1	2.5 ± 0.0
PSM	C	2'-Deoxymugineic acid[b]	319.114	M-H+O[-]	0.253	3.5 ± 0.0**	2.3 ± 0.1	2.6 ± 0.1	2.5 ± 0.1	2.5 ± 0.1	2.6 ± 0.1
PSM	C	3''-deamino−3''-oxonicotianamine	301.104	M-H[-]	0.253	4.1 ± 0.0*	2.3 ± 0.3	2.7 ± 0.0	2.7 ± 0.1	2.7 ± 0.2	2.8 ± 0.2
PSM	C	3-Hydroxy-mugineic acid	317.101	M-H2O-H[-]	0.256	2.4 ± 0.1***	1.2 ± 0.1	3.7 ± 0.1	3.1 ± 0.2	3.6 ± 0.2	3.4 ± 0.1
TCA. GD	C	Citric acid[c]	191.019	M-H[-]	0.279	4.4 ± 0.0	4.3 ± 0.1	4.2 ± 0.0***	4.6 ± 0.0	4.2 ± 0.0	4.3 ± 0.1
AAG. AB. GD	C	Glutamic acid	182.995	M+K-2H[-]	0.356	2.8 ± 0.0***	3.1 ± 0.0	3.1 ± 0.0***	2.9 ± 0.0	3.2 ± 0.0**	3.1 ± 0.0
AAG. AB. CM. CF. LB	C	L-Aspartic acid	88.039	M-HCOOH+H [1 +]	0.259	3.5 ± 0.0***	2.3 ± 0.0	3.0 ± 0.0***	2.6 ± 0.0	2.8 ± 0.1	2.7 ± 0.0
LB. CM	C	L-Homoserine	100.04	M-H2O-H[-]	0.253	3.3 ± 0.0***	1.9 ± 0.1	2.6 ± 0.0	2.4 ± 0.1	2.7 ± 0.1	2.5 ± 0.0
CM	C	O-Acetylserine	182.995	M+K-2H[-]	0.356	2.8 ± 0.1	3.1 ± 0.1	3.1 ± 0.0*	2.9 ± 0.1	3.2 ± 0.0	3.1 ± 0.1
AAG. GD. CF. TCA	K	Oxalacetic acid	191.019	M+CH3COO [-]	0.279	4.4 ± 0.0*	4.3 ± 0.0	4.2 ± 0.0***	4.6 ± 0.0	4.2 ± 0.0**	4.3 ± 0.0
AAG. TCA. AB. GD	K	Oxoglutaric acid	191.019	M+HCOO[-]	0.279	4.4 ± 0.0*	4.3 ± 0.0	4.2 ± 0.0***	4.6 ± 0.0	4.2 ± 0.0**	4.3 ± 0.0
CF	O	Sedoheptulose 1.7-bisphosphate	392.998	M+Na[1 +]	0.237	2.8 ± 0.1**	0.6 ± 0.3	3.1 ± 0.0*	2.3 ± 0.1	2.3 ± 0.5	1.8 ± 0.3
GD. CM	C	Serine	88.039	M-H2O+H [1 +]	0.259	3.5 ± 0.0***	2.3 ± 0.1	3.0 ± 0.0***	2.6 ± 0.0	2.8 ± 0.1	2.7 ± 0.0

For pathway, AAG means "Alanine, aspartate and glutamate metabolism"; AB "Arginine biosynthesis"; CF "Carbon fixation"; CM "Cysteine and methionine metabolism"; GD "Glyoxylate and dicarboxylate metabolism"; LB "Lysine biosynthesis"; PSM "Plant secondary metabolites"; TCA "Tricarboxylic acid cycle".
For compound class, C means "Carboxylic acid and derivatives", K "Keto acids and derivatives" and O "Organooxygen compounds).
In tentative annotation: [a]Also matched to L-homoserine; [b]Also matched to 3-epihydroxy-2'-deoxymugineic acid and mugineic acid; [c]Also matched to isocitric acid.
RT: Retention time in minutes.
Asterisks indicate significant differences between ammonium and nitrate treatments (* $p < 0.05$; ** $p < 0.01$; *** $p < 0.001$).

depict the potential involvement of the metabolic traits identified in the quest of increasing ammonium tolerance and use efficiency to increase crops NUE and to boost NH_4^+-based nutrition in agroecosystems.

Funding sources

This work was supported by the Consolidated Groups program (IT1560- 22) of the Basque Government, by MICIN/AEI/10.13039/501100011033 (project PID2020–113385RBI00) co-funded by 'ERDF A way of making Europe'. Targeted metabolic analyses were funded by the Horizon 2020 European Plant Phenotyping Network Transnational Access Program (EPPN2020 grant agreement no. 731013) and by PHENOME (ANR-11-INBS-0012). MdlP held a doctoral scholarship (Conv. 672) associated with COLCIENCIAS (Department of Science, Technology and Innovation of Colombia) and the Department of Magdalena.

CRediT authorship contribution statement

Daniel Marino: Writing – review & editing, Writing – original draft, Supervision, Project administration, Funding acquisition, Conceptualization. **Yves Gibon:** Writing – review & editing, Supervision, Methodology, Funding acquisition. **Marlon De la Peña:** Writing – review & editing, Writing – original draft, Visualization, Methodology, Investigation, Formal analysis, Data curation. **Gaëtan Glauser:** Writing – review & editing, Investigation, Data curation. **Izargi Vega-Mas:** Writing – review & editing, Investigation. **María Begoña González-Moro:** Writing – review & editing, Writing – original draft, Project administration, Funding acquisition, Formal analysis, Conceptualization.

Declaration of Competing Interest

The authors declare that they have no known competing financial interests or personal relationships that could have appeared to influence the work reported in this paper.

Acknowledgements

Seeds were kindly provided by Prof. Pilar Catalán (University of Zaragoza, Spain). The authors also thank SGIker (UPV/EHU, ERDF, UE) for the technical and human support provided.

Appendix A. Supporting information

Supplementary data associated with this article can be found in the online version at doi:10.1016/j.plantsci.2025.112684.

Data availability

Data will be made available on request.

References

D.I. Arnon, Copper enzymes in isolated chloroplasts. Polyphenoloxidase in *Beta vulgaris*, Plant Physiol. 24 (1949) 1–15, https://doi.org/10.1104/pp.24.1.1.
T. Bantan-Polak, M. Kassai, K.B. Grant, A comparison of fluorescamine and naphthalene-2, 3-dicarboxaldehyde fluorogenic reagents for microplate-based detection of amino acids, Anal. Biochem. 297 (2001) 128–136, https://doi.org/10.1006/abio.2001.5338.
Z. Barhoumi, Insights into the growth response and nitrogen accumulation and use efficiency of the Poaceae grass *Brachypodium distachyon* to high nitrogen availability,

Russ. J. Plant Physiol. 64 (2017) 839–844, https://doi.org/10.1134/S1021443717060024.
P. Catalán, J. Müller, R. Hasterok, G. Jenkins, L.A.J. Mur, T. Langdon, A. Betekhtin, D. Siwinska, M. Pimenetel, D. López-Alvarez, Evolution and taxonomic split of model grass *Brachypodium distachyon*, Ann. Bot. 109 (2012) 385–405, https://doi.org/10.1093/aob/mcr294.
I. Coleto, I. Bejarano, A.J. Marín-Peña, J. Medina, C. Rioja, M. Burow, D. Marino, *Arabidopsis thaliana* transcription factors MYB28 and MYB29 shape ammonium stress responses by regulating Fe homeostasis, New Phytol. 229 (2021) 1021–1035, https://doi.org/10.1111/nph.16918.
I. Coleto, A. Marín-Peña, J.A. Urbano-Gámez, A.I. González-Hernández, W. Shi, G. Li, D. Marino, Interaction of ammonium nutrition with essential mineral cations, J. Exp. Bot. 74 (2023) 6131–6144, https://doi.org/10.1093/jxb/erad215.
L.C. David, T. Girin, E. Fleurisson, E. Phommabouth, A. Mahfoudhi, S. Citerne, P. Berquin, F. Daniel-Vedele, S. Ferrario-Méry, Developmental and physiological responses of *Brachypodium distachyon* to fluctuating nitrogen availability, Sci. Rep. 9 (2019) 3824, https://doi.org/10.1038/s41598-019-40569-8.
M. De la Peña, M.B. González-Moro, D. Marino, Providing carbon skeletons to sustain amide synthesis in roots underlines the suitability of *Brachypodium distachyon* for the study of ammonium stress in cereals, AoB Plants 11 (2019) plz029, https://doi.org/10.1093/aobpla/plz029.
M. De la Peña, A.J. Marín-Peña, L. Urmeneta, I. Coleto, J. Castillo-González, S.M. van Liempd, J.M. Falcón-Pérez, A. Álvarez-Fernández, M.B. González-Moro, D. Marino, Ammonium nutrition interacts with iron homeostasis in *Brachypodium distachyon*, J. Exp. Bot. 73 (2022) 263–274, https://doi.org/10.1093/jxb/erab427.
M. De la Peña, T. Poucet, F. Montardit-Tarda, L. Urmeneta, J.A. Urbano-Gámez, C. Cassan, I. Vega-Mas, P. Catalán, I. Igartua, Y. Gibon, M.B. González-Moro, D. Marino, Natural variation in the adjustment of primary metabolism determines ammonium tolerance in the model grass *Brachypodium distachyon.* J. Exp. Bot. 75 (2024) 7237–7253, https://doi.org/10.1093/jxb/erae382.
F. Dubois, T. Tercé-Laforgue, M.B. González-Moro, J.M. Estavillo, R. Sangwan, A. Gallais, B. Hirel, Glutamate dehydrogenase in plants: is there a new story for an old enzyme? Plant Physiol. Biochem. 41 (2003) 565–576, https://doi.org/10.1016/S0981-9428(03)00075-5.
P.J. Eastmond, I.A. Graham, Re-examining the role of the glyoxylate cycle in oilseeds, Trends Plant Sci. 6 (2001) 72–78, https://doi.org/10.1016/s1360-1385(00)01835-5.
A.T. Eprintsev, D.N. Fedorin, A.V. Salnikov, A.U. Igamberdiev, Expression and properties of the glyoxysomal and cytosolic forms of isocitrate lyase in *Amaranthus caudatus* L, J. Plant Physiol. 181 (2015) 1–8, https://doi.org/10.1016/j.jplph.2015.02.014.
Y. Gibon, O.E. Blaesing, J. Hannemann, P. Carillo, M. Höhne, J.H. Hendriks, M. Stitt, A robot-based platform to measure multiple enzyme activities in Arabidopsis using a set of cycling assays: comparison of changes of enzyme activities and transcript levels during diurnal cycles and in prolonged darkness, Plant Cell 16 (2004) 3304–3325, https://doi.org/10.1105/tpc.104.025973.
M.B. González-Moro, I. González-Moro, M. De la Peña, J.M. Estavillo, P.M. Aparicio-Tejo, D. Marino, C. González-Murua, I. Vega-Mas, A multi-species analysis defines anaplerotic enzymes and amides as metabolic markers for ammonium nutrition, Front. Plant Sci. 11 (2021) 632285, https://doi.org/10.3389/fpls.2020.632285.
A.G. Good, P.H. Beatty, Fertilizing nature: A tragedy of excess in the commons, PLoS Biol. 9 (2011) e1001124, https://doi.org/10.1371/journal.pbio.1001124.
M. Guan, T.C. De Bang, C. Pedersen, J.K. Schjoerring, Cytosolic glutamine synthetase Gln1;2 is the main isozyme contributing to GS1 activity and can be up-regulated to relieve ammonium toxicity, Plant Physiol. 171 (2016) 1921–1933, https://doi.org/10.1104/pp.16.01195.
T. Hachiya, J. Inaba, M. Wakazaki, M. Sato, K. Toyooka, A. Miyagi, M. Kawai-Yamada, D. Sugiura, T. Nakagawa, T. Kiba, A. Gojon, H. Sakakibara, Excessive ammonium assimilation by plastidic glutamine synthetase causes ammonium toxicity in *Arabidopsis thaliana*, Nat. Commun. 12 (2021) 4944, https://doi.org/10.1038/s41467-021-25238-7.
IPCC, Climate Change 2014: Mitigation of Climate Change. Contribution of Working Group III to the Fifth Assessment Report of the Intergovernmental Panel on Climate Change, Cambridge University Press, Cambridge, UK and New York, NY, USA, 2014.
G.J. Li, L. Zhang, M. Wang, D. Di, H.J. Kronzucker, W.M. Shi, The Arabidopsis *AMOT1/EIN3* gene plays an important role in the amelioration of ammonium toxicity, J. Exp. Bot. 70 (2019) 1375–1388, https://doi.org/10.1093/jxb/ery457.
G. Li, L. Zhang, J. Wu, Z. Wang, M. Wang, H.J. Kronzucker, W. Shi, Plant iron status regulates ammonium-use efficiency through protein N-glycosylation, Plant Physiol. 195 (2024) 1712–1727, https://doi.org/10.1093/plphys/kiae103.
G. Li, L. Zhang, J. Wu, X. Yue, M. Wang, L. Sun, D. Di, H.J. Kronzucker, W. Shi, OsEIL1 protects rice growth under NH_4^+ nutrition by regulating OsVTC1-3-dependent N-glycosylation and root NH_4^+ efflux, Plant Cell Environ. 45 (2022) 1537–1553, https://doi.org/10.1111/pce.14283.
S. Li, Y. Park, S. Duraisingham, F.H. Strobel, N. Khan, Q.A. Soltow, D.P. Jones, B. Pulendram, Predicting network activity from high throughput metabolomics, PLoS Comput. Biol. 9 (2013) e1003123, https://doi.org/10.1371/journal.pcbi.1003123.
Y. Liu, R.A. Maniero, R.F.H. Giehl, M. Melzer, P. Steensma, G. Krouk, T.B. Fitzpatrick, N. von Wirén, PDX1.1-dependent biosynthesis of vitamin B6 protects roots from ammonium-induced oxidative stress, Mol. Plant 15 (2022a) 820–839, https://doi.org/10.1016/j.molp.2022.01.012.
Y. Liu, N. von Wirén, Ammonium as a signal for physiological and morphological responses in plants, J. Exp. Bot. 68 (2017) 2581–2592, https://doi.org/10.1093/jxb/erx086.
X.X. Liu, H.H. Zhang, Q.Y. Zhu, J.Y. Ye, Y.X. Zhu, X.T. Jing, W.X. Du, M. Zhou, X.Y. Lin, S.J. Zheng, C.W. Jin, Phloem iron remodels root development in response to ammonium as the major nitrogen source, Nat. Commun. 13 (2022b) 561, https://doi.org/10.1038/s41467-022-28261-4.
D. López-Álvarez, H. Zubair, M. Beckmann, J. Draper, P. Catalán, Diversity and association of phenotypic and metabolomic traits in the close model grasses *Brachypodium distachyon*, *B. stacei* and *B. hybridum*, Ann. Bot. 119 (2017) 545–561, https://doi.org/10.1093/aob/mcw239.
A.J. Marín-Peña, I. Vega-Mas, I. Busturia, C. de la Osa, M.B. González-Moro, J. A. Monreal, D. Marino, Root phosphoenolpyruvate carboxylase activity is essential for *Sorghum bicolor* tolerance to ammonium nutrition, Plant Physiol. Biochem. 206 (2024) 108312, https://doi.org/10.1016/j.plaphy.2023.108312.
D. Marino, J.F. Moran, Can ammonium stress be positive for plant performance? Front. Plant Sci. 10 (2019) 1103, https://doi.org/10.3389/fpls.2019.01103.
L.M. Martínez, A. Fernández-Ocaña, P.J. Rey, T. Salido, F. Amil-Ruiz, A.J. Manzaneda, Variation in functional responses to water stress and differentiation between natural allopolyploid populations in the *Brachypodium distachyon* species complex, Ann. Bot. 121 (2018) 1369–1382, https://doi.org/10.1093/aob/mcy037.
Z. Pang, Y. Lu, G. Zhou, F. Hui, L. Xu, C. Viau, A. Spigelman, P. MacDonald, D. Wishart, S. Li, J. Xia, MetaboAnalyst 6.0: towards a unified platform for metabolomics data processing, analysis and interpretation, Nucleic Acids Res. 52 (2024) 398–406, https://doi.org/10.1093/nar/gkae253.
K. Patterson, T. Cakmak, A. Cooper, I. Lager, A.G. Rasmusson, M.A. Escobar, Distinct signalling pathways and transcriptome response signatures differentiate ammonium- and nitrate-supplied plants, Plant Cell Environ. 33 (2010) 1486–1501, https://doi.org/10.1111/j.1365-3040.2010.02158.x.
T. Poucet, M.B. González-Moro, C. Cabasson, B. Beauvoit, Y. Gibon, M. Dieuaide-Noubhani, D. Marino, Ammonium supply induces differential metabolic adaptive responses in tomato according to leaf phenological stage, J. Exp. Bot. 72 (2021) 3185–3199, https://doi.org/10.1093/jxb/erab057.
A.G. Rasmusson, M.A. Escobar, M. Hao, A. Podgórska, B. Szal, Mitochondrial NAD(P)H oxidation pathways and nitrate/ammonium redox balancing in plants, Mitochondrion 53 (2020) 158–165, https://doi.org/10.1016/j.mito.2020.05.010.
A. Rodríguez, H.J.M. van Grinsven, M.P. van Loon, J.C. Doelman, A.H.W. Beusen, L. Lassaletta, Costs and benefits of synthetic nitrogen for global cereal production in 2015 and in 2050 under contrasting scenarios, Sci. Total Environ. 912 (2024) 169357, https://doi.org/10.1016/j.scitotenv.2023.169357.
J. Sánchez-Zabala, C. González-Murua, D. Marino, Mild ammonium stress increases chlorophyll content in *Arabidopsis thaliana*, Plant Signal. Behav. 10 (2015) e991596, https://doi.org/10.4161/15592324.2014.991596.
A. Sarasketa, M.B. González-Moro, C. González-Murua, D. Marino, Exploring ammonium tolerance in a large panel of *Arabidopsis thaliana* natural accesions, J. Exp. Bot. 65 (2014) 6023–6033, https://doi.org/10.1093/jxb/eru342.
K.B.G. Scholthof, S. Irigoyen, P. Catalan, K.K. Mandadi, *Brachypodium*: a monocot grass model genus for plant biology, Plant Cell 30 (2018) 1673–1694, https://doi.org/10.1105/tpc.18.00083.
G.V. Subbarao, T.D. Searchinger, A 'more ammonium solution' to mitigate nitrogen pollution and boost crop yields, Proc. Natl. Acad. Sci. USA 118 (2021) e2107576118, https://doi.org/10.1073/pnas.2107576118.
K. Takahagi, K. Inoue, M. Shimizu, Y. Uehara-Yamaguchi, Y. Onda, K. Mochida, Homoeolog-specific activation of genes for heat acclimation in the allopolyploid grass *Brachypodium hybridum*, GigaScience 7 (2018) giy020, https://doi.org/10.1093/gigascience/giy020.
L. Tyler, S.J. Lee, N.D. Young, G.A. DeIulio, E. Benavente, M. Reagon, J. Sysopha, R. M. Baldini, A. Troìa, S.P. Hazen, A.L. Caicedo, Population structure in the model grass *Brachypodium distachyon* is highly correlated with flowering differences across broad geographic areas, Plant Genome 9 (2016) 777–780, https://doi.org/10.3835/plantgenome2015.08.0074.
I. Vega-Mas, M.T. Rossi, K.J. Gupta, C. González-Murua, R.G. Ratcliffe, J.M. Estavillo, M. B. González-Moro, Tomato roots exhibit in vivo glutamate dehydrogenase aminating capacity in response to excess ammonium supply, J. Plant Physiol. 239 (2019) 83–91, https://doi.org/10.1016/j.jplph.2019.03.009.
C. Xiao, Y. Fang, S. Wang, K. He, The alleviation of ammonium toxicity in plants, J. Integr. Plant Biol. 65 (2023) 1362–1368, https://doi.org/10.1111/jipb.13467.
J. Wang, N. Hüner, L. Tian, Identification and molecular characterization of the *Brachypodium distachyon NRT2* family, with a major role of *BdNRT2. 1*, Physiol. Plant 165 (2019) 498–510, https://doi.org/10.1111/ppl.12716.